

# The Art of Filling Protein Pockets Efficiently with Octahedral Metal Complexes\*\*

Sebastian Blanck, Jasna Maksimoska, Julia Baumeister, Klaus Harms, Ronen Marmorstein,\* and Eric Meggers\*

Complicated natural products whose structures and properties have evolved over millions of years frequently display specific biological modes of action that can often be traced back to their preorganized three-dimensional structures which perfectly complement the shape and functional-group presentation of their target protein pockets.<sup>[1]</sup> A recent study analyzed the protein-binding properties of compounds from natural as well as synthetic sources and found that the protein-binding selectivity correlated with the shape complexity (defined as the relative number of  $sp^3$ -hybridized carbon atoms) and the stereochemical complexity (defined as the relative number of stereogenic carbons).<sup>[2]</sup> Octahedral metal complexes may offer an attractive alternative to sophisticated globular and rigid structural templates. They are constructed from a single metal stereocenter and chelating ligands limit the degree of conformational flexibility; thus “natural-product-like” structural complexities and strikingly high target specificities are achieved, as our group has demonstrated in several previous studies.<sup>[3–6]</sup>

An important aspect in the design of such metal-templated protein binders not articulated in the past is the three-dimensional space requirement of an octahedral center. This is a crucial aspect of the inhibitor design, mainly because the metal must be located at a specific position within the active site in order to be useful. For example, if the metal is located too far within the active site or too close to the protein backbone there will not be enough space available to accommodate the octahedral coordination sphere. In contrast, if the metal is located too close to the solvent, the metal center cannot easily impact binding affinity and selectivity. A clear indicator for an advantageous metal position within the protein pocket is the strong influence of the metal coordination sphere on the binding affinity and selectivity. We have identified such a privileged position of the metal within the ATP-binding site of protein kinases by using the well-established staurosporine-inspired metallopyridocarbazole

scaffold.<sup>[3–7]</sup> For example, the octahedral organoruthenium complex  $\Lambda$ -FL172 was designed as a selective inhibitor for the p21-activated kinase 1 (PAK1),<sup>[8]</sup> in which the bidentate pyridocarbazole ligand of the ruthenium complex occupies the adenine pocket (Figure 1).<sup>[4]</sup> By interacting with the so-called hinge region it places the ruthenium center at a defined position within the ribose binding site, where the additional CO, chloride, and bidentate iminopyridine ligands can form important contacts with other parts of the active site and thereby strongly contribute to binding the affinity and selectivity.<sup>[4,6]</sup>

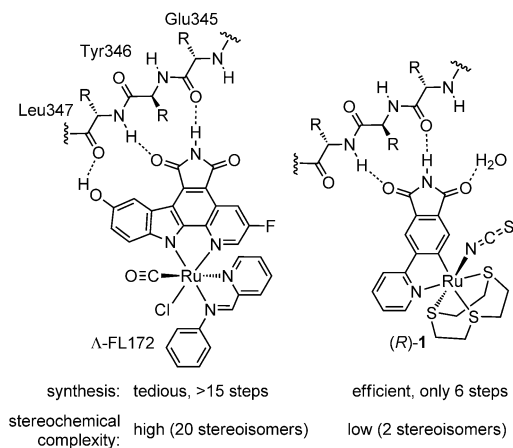


**Figure 1.** Comparison of two strategies for the design of metal-templated inhibitors of the protein kinase PAK1.

In order to better understand the design of metal-based enzyme inhibitors, we wondered whether this design is unique or whether other scaffolds with metals located at different positions within the active site could yield similar or even better results. To address this question, we designed new scaffolds<sup>[9]</sup> and discovered the simple ruthenium complex (*R*)-**1**, which places the metal at a distinct position within the ATP-binding site, contains a completely different set of coordinating ligands, and yet shows an improved affinity for PAK1 compared to that of the much more complicated pyridocarbazole complex  $\Lambda$ -FL172.

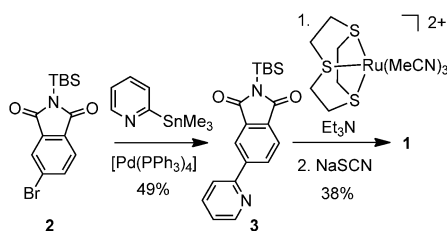
Ruthenium complex **1** is based on a simple pyridylphthalimide scaffold, which can be synthesized in just a few steps (Scheme 1). Accordingly, a Suzuki cross-coupling of bromophthalimide **2** with 2-trimethylstannylpyridine afforded the pyridylphthalimide **3** (49%), which was sub-

[\*] S. Blanck, Dr. K. Harms, Prof. Dr. E. Meggers  
Fachbereich Chemie, Philipps-Universität Marburg  
Hans-Meerwein-Strasse, 35043 Marburg (Germany)  
E-mail: meggers@chemie.uni-marburg.de

Dr. J. Maksimoska, Prof. R. Marmorstein  
The Wistar Institute  
3601 Spruce Street, Philadelphia, PA 19104 (USA)  
E-mail: marmor@wistar.org

[\*\*] This work was supported by the German Research Foundation (DFG) and the U.S. National Institutes of Health (CA114046). S.B. acknowledges a stipend from the Fonds der Chemischen Industrie.

Supporting information for this article is available on the WWW under <http://dx.doi.org/10.1002/anie.201108865>.



**Scheme 1.** Synthesis of pyridylphthalimide ruthenium complex **1**. TBS = *tert*-butyldimethylsilyl.

sequently reacted with the ruthenium complex  $[\text{Ru}(\text{C}_6\text{H}_{12}\text{S}_3)(\text{MeCN})_3](\text{CF}_3\text{SO}_3)_2$  under basic conditions, followed by the addition of NaSCN to afford the racemic complex **1** (38% over two steps). A crystal structure of the N-benzylated derivative of **1** is shown in Figure 2 and indicates the formation of a C–Ru bond. This cyclometalation reduces the requirement for metal-coordinating heteroatoms and is thus crucial for the short and efficient synthesis.

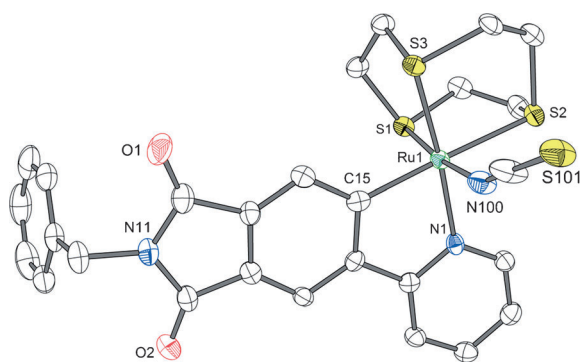


**Figure 2.** Structure of the N-benzylated derivative of complex **1**. Disordered solvent molecules and a disordered position of S101 are not shown. Thermal ellipsoids drawn at 50% probability level. Selected bond lengths [Å]: C15–Ru1 = 2.033(4), N1–Ru1 = 2.098(3), N100–Ru1 = 2.084(3), S1–Ru1 = 2.2770(9), S2–Ru1 = 2.3972(9), S3–Ru1 = 2.2923(9).

The racemic complex **1** displays an  $\text{IC}_{50}$  value of  $(83 \pm 20)$  nM ( $1 \mu\text{M}$  ATP) against PAK1 (Figure 3), which is slightly more potent than the previously reported  $\Lambda$ -FL172 ( $\text{IC}_{50} = 130$  nM,  $1 \mu\text{M}$  ATP).<sup>[4]</sup> Interestingly, the pyridylphthalimide ligand itself is not an inhibitor of PAK1 ( $\text{IC}_{50} > 100 \mu\text{M}$ ), thus the entire coordination sphere is important for protein kinase binding.

PAK1 contains an atypical, open ATP-binding site which is probably responsible for the difficulties in developing high-affinity inhibitors of this kinase.<sup>[4,8,10]</sup> A cocrystal structure at a resolution of 2.0 Å reveals the binding of the *R* enantiomer of **1** to the ATP binding site of PAK1 (amino acids 249–545 with mutation Lys299Arg;<sup>[11]</sup> Figures 4 and 5). The van der Waals surface representation shown in Figure 4 demonstrates how nicely the ATP-binding site is filled with (*R*)-**1** in a shape-complementary fashion with the phthalimide moiety additionally forming two hydrogen bonds with the hinge region (Glu345 and Leu347) and one water-mediated contact to

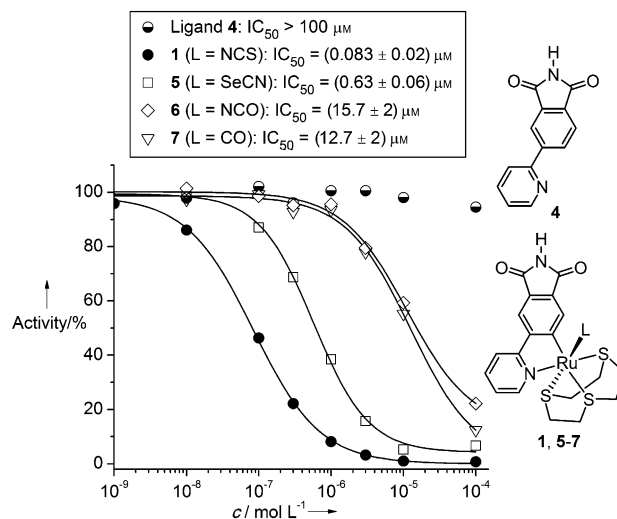


**Figure 3.**  $\text{IC}_{50}$  curves of ligand **4**, complex **1**, and complexes **5–7** with PAK1. ATP concentration was  $1 \mu\text{M}$ .

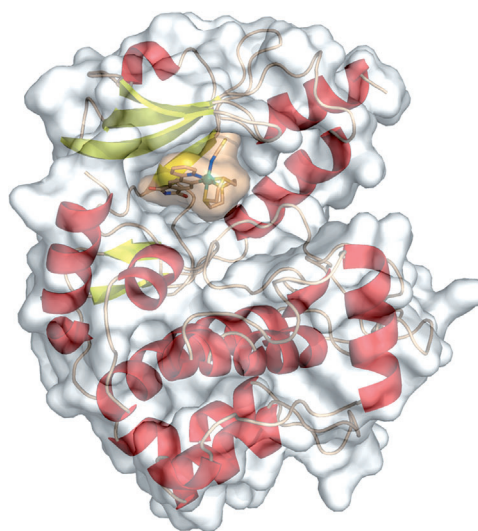


**Figure 4.** Cocrystal structure of PAK1 (amino acids 249–545 with mutation Lys299Arg) and (*R*)-**1** at a resolution of 2.0 Å; the van der Waals surfaces are displayed. Coordinates of the structure have been deposited in the Protein Data Bank (PDB ID: 4DAW).

Thr406 (Figure 5). Interestingly, superimposition of this structure with the recently disclosed PAK1/ $\Lambda$ -FL172<sup>[4]</sup> cocrystal structure demonstrates that even though both compounds are ATP-competitive binders, they significantly differ in their binding modes (Figure 6). While both form the canonical hydrogen bonds between the maleimide moieties of the inhibitor and the hinge region of the kinase, the aromatic heterocycles are rotated towards each other by approximately 30° demonstrating the range that is possible for the directionality of hydrogen bonds. Furthermore, the metal centers of the two inhibitor scaffolds are 3.0 Å apart from each other and the monodentate ligands point into different areas of the active site. Whereas the CO ligand of FL172 is located right below the center of the glycine-rich loop (P-loop), the NCS

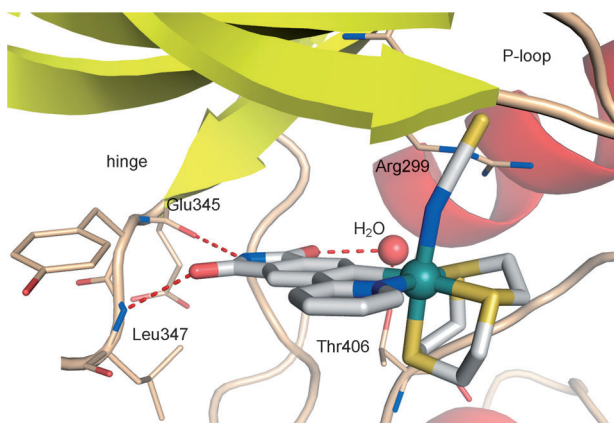


**Figure 5.** Hydrogen bonding of (R)-1 within the ATP-binding site of PAK1.

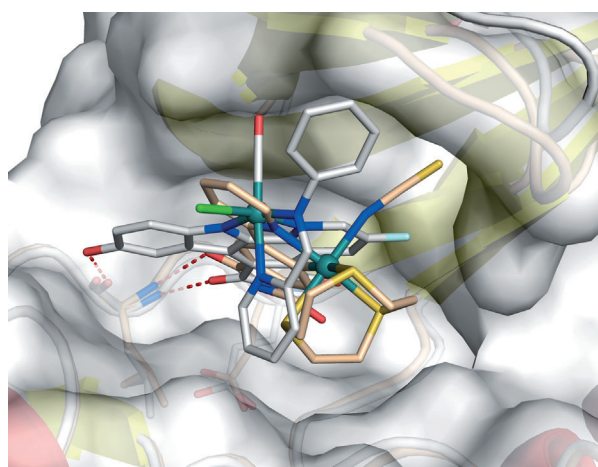


**Figure 6.** Relative binding position of (R)-1 and Δ-FL172 (PDB ID: 3FXZ) within the ATP-binding site of PAK1. Superimposed with the PyMOL Molecular Graphics System, Version 1.3, Schrödinger, LLC.

ligand of **1** points towards the interface of the glycine-rich loop (connecting strands  $\beta 1$  and  $\beta 2$ ) and the methylene groups of Arg299 of the  $\beta$ -sheet strand  $\beta 3$ , thereby perfectly filling a small hydrophobic pocket as visualized in the van der Waals representation of Figure 4. The importance of the NCS ligand is manifested by the loss of the binding affinity of related complexes, which carry a SeCN ( $IC_{50} = (0.625 \pm 0.06) \mu M$ , 7.5-fold weaker inhibitor), NCO ( $IC_{50} = (15.7 \pm 2) \mu M$ , 193-fold weaker inhibitor), or CO ligand instead ( $IC_{50} = (12.7 \pm 2) \mu M$ , 153-fold weaker inhibitor) (Figure 3). This intriguing example demonstrates how a change in the position of the metal within the active site, even if it is just shifted by 3.0 Å, requires a completely different coordination sphere to fill the protein pocket in a comparable fashion.

In conclusion, the design of a metal-based enzyme inhibitor described here along with the crystallographic analysis of its binding within the enzyme active site emphasize the broad range of possibilities for fitting octahedral metal

complexes in an enzyme active site. Despite the brevity of the synthesis (overall only six steps) and simplicity of the structure (only two stereoisomers possible), complex **1** displays an  $IC_{50}$  value of 83 nM (1  $\mu M$  ATP), which is superior to that of FL172, a complex that is much more tedious to synthesize (> 15 steps) and of higher stereochemical complexity (20 possible stereoisomers). To date, the ruthenium phthalimide complex **1** described is among the most potent ATP-competitive inhibitors known for the protein kinase PAK1,<sup>[12]</sup> demonstrating the advantages of filling large or open pockets with globular octahedral metal complexes.

Received: December 16, 2011

Published online: March 1, 2012

**Keywords:** bioorganometallic chemistry · enzyme inhibitors · protein kinases · ruthenium

- [1] E. E. Carlson, *ACS Chem. Biol.* **2010**, *5*, 639–653.
- [2] P. A. Clemons, N. E. Bodycombe, H. A. Carrinski, J. A. Wilson, A. F. Shamji, B. K. Wagner, A. N. Koehler, S. L. Schreiber, *Proc. Natl. Acad. Sci. USA* **2010**, *107*, 18787–18792.
- [3] H. Bregman, P. J. Carroll, E. Meggers, *J. Am. Chem. Soc.* **2006**, *128*, 877–884.
- [4] J. Maksimoska, L. Feng, K. Harms, C. Yi, J. Kissil, R. Marmorstein, E. Meggers, *J. Am. Chem. Soc.* **2008**, *130*, 15764–15765.
- [5] A. Wilbuer, D. H. Vlecken, D. J. Schmitz, K. Kräling, K. Harms, C. P. Bagowski, E. Meggers, *Angew. Chem.* **2010**, *122*, 3928–3932; *Angew. Chem. Int. Ed.* **2010**, *49*, 3839–3842.
- [6] L. Feng, Y. Geisselbrecht, S. Blanck, A. Wilbuer, G. E. Atilla-Gokcumen, P. Filippakopoulos, K. Kräling, M. A. Celik, K. Harms, J. Maksimoska, R. Marmorstein, G. Frenking, S. Knapp, L.-O. Essen, E. Meggers, *J. Am. Chem. Soc.* **2011**, *133*, 5976–5986.
- [7] E. Meggers, G. E. Atilla-Gokcumen, H. Bregman, J. Maksimoska, S. P. Mulcahy, N. Pagano, D. S. Williams, *Synlett* **2007**, 1177–1189.
- [8] The p21-activated kinases are important mediators of signaling pathways that regulate cellular processes and are implicated in pathological conditions including cancer. See, for example: C. Yi, J. Maksimoska, R. Marmorstein, J. L. Kissil, *Biochem. Pharmacol.* **2010**, *80*, 683–689.
- [9] Other designs of metal-based kinase inhibitors: a) J. Spencer, A. P. Mendham, A. K. Kotha, S. C. W. Richardson, E. A. Hillard, G. Jaouen, L. Male, M. B. Hursthouse, *Dalton Trans.* **2009**, 918–921; b) B. Biersack, M. Zoldakova, K. Effenberger, R. Schobert, *Eur. J. Med. Chem.* **2010**, *45*, 1972–1975; c) S. Blanck, T. Cruchter, A. Vultur, R. Riedel, K. Harms, M. Herlyn, E. Meggers, *Organometallics* **2011**, *30*, 4598–4606.
- [10] a) M. Lei, W. Lu, W. Meng, M.-C. Parrini, M. J. Eck, B. J. Mayer, S. C. Harrison, *Cell* **2000**, *102*, 387–397; b) M. Lei, M. A. Robinson, S. C. Harrison, *Structure* **2005**, *13*, 769–778.
- [11] The lysine-to-arginine mutation at position 299 inactivates the enzyme but is important for the large-scale cellular expression of PAK1 for crystallization purposes. However, this mutation apparently does not lead to any significant structural changes. See Ref. [10].
- [12] See the Supporting Information for a kinase selectivity profile of **1**.